EVALUATING THE SHORT ENCOUNTER ASSUMPTION OF THE PROBABILITY OF COLLISION FORMULA

Vincent T. Coppola[*]

The formula for the probability of collision for space objects results from many assumptions concerning the motion of the objects, not least of which is that the encounter duration is short. We develop a formula that characterizes the encounter duration for the conjunction of two space objects and then compute it for every conjunction in an all-on-all assessment of the public catalog. We then introduce the concept of a short-term encounter validity interval that characterizes the total encounter time under which the short-term assumptions are assumed met. This metric provides the means for assessing whether a conjunction satisfies the short encounter assumption so that the standard collision probability metric is valid.

INTRODUCTION

The formula for the probability of collision for space objects results from many assumptions concerning the motion of the objects, not least of which is that the encounter duration is short. Certainly, the expectation is that most encounter times are indeed short because space objects move at speeds measured in km/sec. However, not every encounter will be of short duration. Two obvious examples are (i) conjunctions involving objects flying in formation close to one another; and (ii) conjunctions involving objects at GEO that slowly drift. Since the formula rests upon a short time assumption, its use requires a determination that the assumption is indeed met. More importantly, the formula should not be used when the assumption is violated.

There have been many papers describing the probability of collision formula: see Alfano,[1,2,3] Chan,[4,5,6,7,8] and Patera[9] for example. The formula involves the integration of a Gaussian probability density function over a circular area in the encounter plane. The encounter plane is defined as the plane perpendicular to the relative velocity vector between the two objects at TCA (i.e., time of closest approach). The formula was first described by Foster and Estes.[10]

A first principles approach to the derivation of the formula was taken by Akella and Alfriend[11] and by Coppola.[12] They showed that a probability computation involving the 3-dimensional relative position covariance reduces to a 2-dimensional area computation by integrating out the motion over time. While Akella and Alfriend integrate over all time, the integrand approaches zero exponentially so that only a finite duration is actually needed to well-approximate the integral as one. The short encounter time assumption needs to hold only over this finite duration.

Others have developed tests for determining when the short encounter assumption is valid. Alfano[13] developed a linearity test that determines a minimum relative velocity at TCA so that a user-specified encounter distance (expressed in standard deviations) is traversed without altering the

[*]Sr. Astrodynamics Developer, Analytical Graphics Inc., 220 Valley Creek Blvd, Exton PA, 19341.

probability value by a user-specified fractional tolerance. Chan[7] argues for an encounter distance, measured in standard deviations, that makes the cumulative probability normal to the encounter plane the value one to within machine precision. Frigm and Rohrbaugh[14] investigated the use of relative velocity as an indicator of long vs. short term encounters for a select set of LEO and GEO spacecraft.

We will investigate the appropriateness of the short encounter assumption by computing the encounter duration for every conjunction in an all-on-all assessment of a large public catalog of space objects. We will show that the short encounter assumption is not valid for certain conjunctions while being appropriate for the vast majority. The computation of the encounter duration provides a means for assessing the appropriateness of the collision probability formula.

DERIVATION

The classic short encounter formula for the probability of collision between space objects has been derived by many authors.[10, 15, 1, 4, 11, 12] The probability represents the likelihood that the range between two objects becomes less than the radius R during the encounter time interval, where R is usually taken to be the sum of the hard body radii of the two objects involved. Because of this definition, the probability does not represent the likelihood of a collision at any particular value of time. Instead, the probability is associated with the whole time interval of the encounter.

Short-term Encounter Formula

In its most general form, the probability of collision formula is a two-dimensional integral of a Gaussian distribution in the encounter plane over the area of a circle of radius R:

$$P = \iint\limits_{|\boldsymbol{\zeta}| \leq R} \mathcal{N}_2(\boldsymbol{\zeta}, \boldsymbol{\mu}_{\zeta_0}, \mathbf{P}_c) d\boldsymbol{\zeta} \, , \tag{1}$$

where $\boldsymbol{\zeta} = (y, z)$ denotes random variables for the relative position vector in the encounter plane, $\boldsymbol{\mu}_{\zeta_0}$ denotes the mean value of $\boldsymbol{\zeta}$, and $\mathbf{P}_c$ denotes the 2×2 covariance matrix for $\boldsymbol{\zeta}$ about $\boldsymbol{\mu}_{\zeta_0}$. The expression $\mathcal{N}_n(\boldsymbol{\xi}, \boldsymbol{\eta}, \mathbf{P})$ denotes the normal (Gaussian) distribution for an n-dimensional variable $\boldsymbol{\xi}$ with mean $\boldsymbol{\eta}$ and symmetric positive-definite $n \times n$ covariance matrix $\mathbf{P}$ defined by

$$\mathcal{N}_n(\boldsymbol{\xi}, \boldsymbol{\eta}, \mathbf{P}) = \frac{1}{\sqrt{(2\pi)^n}} \frac{1}{\sqrt{\det \mathbf{P}}} \exp\left[-\frac{1}{2} \left(\boldsymbol{\xi} - \boldsymbol{\eta} \right)^T \mathbf{P}^{-1} \left(\boldsymbol{\xi} - \boldsymbol{\eta} \right) \right] \, . \tag{2}$$

One object is termed the primary object while the other is termed the secondary object. The encounter plane is defined as the plane containing the primary object's position whose normal is aligned with the relative velocity vector between the objects at TCA. With (y, z) parameterizing the plane, the normal becomes $\hat{\mathbf{i}}$. The choice of the plane makes the relative position vector at TCA lie in the encounter plane, denoted $\boldsymbol{\mu}_{\zeta_0}$ above.

Several assumptions have been made in deriving Eq. (1). First, the encounter occurs over so small a time interval that the motion of the objects can be assumed to be linear (i.e., straight lines). Second, the velocity uncertainty is assumed to be sufficiently small that it can be treated as zero and ignored. Thus, all perturbed relative trajectories are parallel and have the same identical constant velocity while still having uncertainty in relative position. The mean relative motion is expressed as

$$\mu_x(t) = \mu_{x_0} + v_0(t - t_0) \, , \tag{3a}$$

$$\mu_y(t) = \mu_{y_0} , \tag{3b}$$

$$\mu_z(t) = \mu_{z_0} . \tag{3c}$$

Trajectories for a sphere of initial conditions of radius R, centered on the mean trajectory, sweeps out a cylinder over time, often referred to as the collision tube. Given the linear motion assumption, only trajectories starting within the tube can ever collide; no trajectory outside the tube ever crosses inside.

The probability density functions for both objects are assumed to be independent and Gaussian for times near TCA. The linear motion and velocity uncertainty assumptions further render the covariance constant as well. The two-dimensional probability density function in the encounter plane $\mathbf{P}_c$ is found by summing the 3×3 position covariance matrices of the two objects at TCA, rotating the components into axes created by the plane and its normal, and then extracting the 2×2 sub-matrix $\mathbf{P}_c$ from it.

Identifying the Encounter Interval

The formula given by Eq. (1) has no information in it concerning the encounter time interval. Akella and Alfriend[11] were the first to show that Eq. (1) is derivable from more fundamental notions involving a 3-dimensional integral of the full 3×3 relative position covariance matrix. The integral over the dimension perpendicular to the encounter plane could be associated with an integral over time. Integrating over all time is then equivalent to integrating the entire normal distribution resulting in a value of 1. The remaining 2 dimensions were then given by Eq. (1).

A rigorous derivation of the probability of collision formula, including the effects of relative velocity uncertainty, is given by Coppola.[12] The probability of collision P is the sum of the initial probability of collision P_0 at the start time t_0 of the encounter time interval and the probability P_I that trajectories will have a collision after t_0 but within a duration $T > 0$. By choosing the initial time t_0 sufficiently earlier than the TCA, P_0 can be made approximately zero for many types of encounters.* In fact, the short encounter assumption assumes that such an initial time t_0 can be found. The probability P_I involves a time integral, given by

$$P_I = \int_{t_0}^{t_0+T} \iint_{|\boldsymbol{\zeta}| \leq R} \mathcal{N}_3(\mathbf{r}, \boldsymbol{\mu}_r, \mathbf{A}_0) v_0 \, dydzdt . \tag{4}$$

where v_0 is the relative speed at TCA, $\mathbf{r} = (x, \boldsymbol{\zeta})$ is the relative position, $\boldsymbol{\mu}_r = (\mu_x, \boldsymbol{\mu}_{\zeta_0})$, $\mathbf{A}_0$ is the 3×3 relative position covariance matrix, and the (x, y, z) axes have been chosen to align the relative velocity at TCA with the positive x-axis. When evaluating Eq. (4), $x = -\sqrt{R^2 - \boldsymbol{\zeta}^T \boldsymbol{\zeta}}$ so that $\mathbf{r}$ lies on the correct hemisphere of radius R, a fundamental notion of the derivation. Eq. (4) is equivalent to Akella and Alfriend's Eq.(28) when $t_0 + T \to \infty$ and $t_0 \to -\infty$.

The reduction of Eq. (4) to Eq. (1) follows by first decomposing the 3-dimensional normal distribution into a product of terms that preserves the covariance in the encounter plane:[11, 12]

$$\mathcal{N}_3(\mathbf{r}, \boldsymbol{\mu}_r, \mathbf{A}_0) = \mathcal{N}_1(x - \mathbf{b}^T \boldsymbol{\zeta}, \mu_x - \mathbf{b}^T \boldsymbol{\mu}_{\zeta_0}, \sigma_\nu^2) \mathcal{N}_2(\boldsymbol{\zeta}, \boldsymbol{\mu}_{\zeta_0}, \mathbf{P}_c) , \tag{5}$$

---

*Objects flying in formation or objects having long encounters may not be able to choose an initial time t_0 to make $P_0 \approx 0$.

where $\sigma_\nu^2 = \eta^2 - \mathbf{b}^T \mathbf{w}$, $\mathbf{b}^T = \mathbf{w}^T \mathbf{P}_c^{-1}$, and

$$\mathbf{A}_0 = \left| \begin{array}{cc} \eta^2 & \mathbf{w}^T \\ \mathbf{w} & \mathbf{P}_c \end{array} \right| \quad \eta \in \mathbb{R}, \mathbf{w} \in \mathbb{R}^2 . \tag{6}$$

Note that the second normal distribution in Eq. (5) is independent of time t. The probability integral is then

$$P_I = \iint\limits_{|\boldsymbol{\zeta}| \leq R} \mathcal{N}_2(\boldsymbol{\zeta}, \boldsymbol{\mu}_{\zeta_0}, \mathbf{P}_c) \int\limits_{t_0}^{t_0+T} \mathcal{N}_1(x - \mathbf{b}^T \boldsymbol{\zeta}, \mu_x - \mathbf{b}^T \boldsymbol{\mu}_{\zeta_0}, \sigma_\nu^2) \, v_0 \, dt \, d\boldsymbol{\zeta} . \tag{7}$$

The inner integral is an integral over time t, treating $\boldsymbol{\zeta}$ as a parameter, where the only time dependence lies in μ_x. If we let $t = 0$ represent the TCA, then $\mu_x(0) = 0$ making $\mu_{x_0} = v_0 t_0$ and the inner integral becomes

$$P_\nu(\boldsymbol{\zeta}) = \int\limits_{t_0}^{t_0+T} \mathcal{N}_1 \, v_0 \, dt = \int\limits_{\chi_0}^{\chi_T} \mathcal{N}_1(\chi, 0, \sigma_\nu^2) \, d\chi , \tag{8a}$$

$$\text{where } \chi = v_0 t + \mathbf{b}^T(\boldsymbol{\zeta} - \boldsymbol{\mu}_{\zeta_0}) + \sqrt{R^2 - \boldsymbol{\zeta} \cdot \boldsymbol{\zeta}} . \tag{8b}$$

Encounter Duration

While $P_\nu(\boldsymbol{\zeta})$ is 1 when integrating over all time, it can be accurately approximated as 1 when integrating over a finite duration. We define this duration as the short-term encounter duration. Eq. (8a) can be integrated analytically as

$$P_\nu(\boldsymbol{\zeta}) = \frac{1}{2} \left(\mathrm{erf}(\alpha_T) - \mathrm{erf}(\alpha_0) \right) , \tag{9}$$

where $\alpha_T = \alpha_0 + \alpha_\tau$ and

$$\alpha_\tau = \frac{v_0 T}{\sqrt{2}\sigma_\nu} , \tag{10a}$$

$$\alpha_0 = \frac{v_0 t_0 - q_0 + \delta(\boldsymbol{\zeta})}{\sqrt{2}\sigma_\nu} , \tag{10b}$$

$$q_0 = \mathbf{b}^T \boldsymbol{\mu}_{\zeta_0} , \tag{10c}$$

$$\delta(\boldsymbol{\zeta}) = \mathbf{b}^T \boldsymbol{\zeta} + \sqrt{R^2 - \boldsymbol{\zeta}^T \boldsymbol{\zeta}} . \tag{10d}$$

$P_\nu(\boldsymbol{\zeta}) \to 1$ when both $\mathrm{erf}(\alpha_T) \to 1$ and $\mathrm{erf}(\alpha_0) \to -1$. Define the measure of closeness to 1 using $1 - \gamma$ where $\gamma > 0$ but small. Define α_c by $\mathrm{erfc}(\alpha_c) = \gamma$. Table 1 shows the relationship between γ and α_c. Note that α_c increases slowly as γ becomes smaller. On a computer, the resolution of a double is nearly 1.e-16, so γ values less than that are not meaningful to compute.

Looking first at α_0, we find

$$\mathrm{erf}(\alpha_0) \leq -(1 - \gamma) \quad \text{whenever} \quad \alpha_0 \leq -\alpha_c . \tag{11}$$

This condition is satisfied when $t_0 \leq \tau_0$ where

$$\tau_0 = \frac{-\sqrt{2}\alpha_c\sigma_\nu + q_0 - \delta_{max}}{v_0} \quad \text{where} \quad \delta_{max} = \max_{\|\boldsymbol{\zeta}\| \leq R} \delta(\boldsymbol{\zeta}) . \tag{12}$$

4

Table 1. Relating γ to the sigma value α_c

γ	α_c	$\sqrt{2}\alpha_c$	$2\sqrt{2}\alpha_c$
1.0e-06	3.459	4.892	9.783
1.0e-08	4.052	5.731	11.461
1.0e-10	4.573	6.467	12.934
1.0e-12	5.042	7.131	14.261
1.0e-14	5.473	7.739	15.479
1.0e-16	5.864	8.292	16.585

Similarly, we find

$$\text{erf}(\alpha_T) \geq (1-\gamma) \quad \text{whenever} \quad \alpha_T \geq \alpha_c. \tag{13}$$

This condition is satisfied when $(t_0 + T) \geq \tau_1$ where

$$\tau_1 = \frac{\sqrt{2}\alpha_c\sigma_\nu + q_0 - \delta_{min}}{v_0} \quad \text{where} \quad \delta_{min} = \min_{\|\boldsymbol{\zeta}\| \leq R} \delta(\boldsymbol{\zeta}). \tag{14}$$

The encounter duration is computed as $\Delta\tau = \tau_1 - \tau_0$. Direct computation shows that the minimum and maximum of $\delta(\boldsymbol{\zeta})$ over the area of the circle $\|\boldsymbol{\zeta}\| \leq R$ are

$$\delta_{min} = -R\sqrt{\mathbf{b}^T\mathbf{b}} \quad \text{at} \quad \boldsymbol{\zeta} = -\frac{R\mathbf{b}}{\sqrt{\mathbf{b}^T\mathbf{b}}}, \tag{15a}$$

$$\delta_{max} = R\sqrt{1 + \mathbf{b}^T\mathbf{b}} \quad \text{at} \quad \boldsymbol{\zeta} = \frac{R\mathbf{b}}{\sqrt{1 + \mathbf{b}^T\mathbf{b}}}. \tag{15b}$$

The minimum occurs in the encounter plane at $x = 0$ on the boundary of the circle; the maximum occurs at an interior point. Substituting, we find

$$\tau_0(\gamma) = \frac{-\sqrt{2}\alpha_c(\gamma)\sigma_\nu + q_0 - R\sqrt{1 + \mathbf{b}^T\mathbf{b}}}{v_0}, \tag{16a}$$

$$\tau_1(\gamma) = \frac{\sqrt{2}\alpha_c(\gamma)\sigma_\nu + q_0 + R\sqrt{\mathbf{b}^T\mathbf{b}}}{v_0}, \tag{16b}$$

$$\Delta\tau(\gamma) = \frac{2\sqrt{2}\alpha_c(\gamma)\sigma_\nu + R\left(\sqrt{1 + \mathbf{b}^T\mathbf{b}} + \sqrt{\mathbf{b}^T\mathbf{b}}\right)}{v_0}. \tag{16c}$$

As expected, the encounter duration is related to the relative speed v_0 at TCA and the relative position uncertainty normal to the encounter plane σ_ν. Note that σ_ν properly accounts for cross-correlation between the uncertainty in encounter plane and uncertainty along its normal. The term multiplying R weights the transversal of the hemisphere itself by the cross-correlation. Usually, $\sigma_\nu \gg R$ so that the σ_ν term dominates $\Delta\tau(\gamma)$. Note also that while choosing different measures of closeness γ will affect $\Delta\tau(\gamma)$, the difference in duration between the smallest and largest γ from Table 1 is only 70% longer.

Chan[7] argues for an encounter duration* of at least $6\sigma v_0$ but preferring $17\sigma v_0$, essentially choosing γ as 1.e-16. Although he does not provide a formula for his σ, his argument is in accordance with the results presented here, assuming that the hemispherical traversal time is a small component to $\Delta\tau(\gamma)$.

---

*Rather than speaking in terms of time, Chan uses distance when reducing the 3 dimensional probability integral to 2 dimensions. These are simply related using v_0.

EVALUATING THE ENCOUNTER DURATION FOR A CATALOG OF SPACE OBJECTS

We want to assess the encounter duration for each conjunction in all-on-all conjunction assessment of the public catalog of space objects. We chose a 2-day time period over 01-03 Oct 2011. However, a high-accuracy space catalog, containing ephemeris and covariance information for all space objects, is not made available to the public. Thus, we resorted to the creation of our own simulated catalog based upon the only the publicly available information for space objects: TLEs.

Simulated Catalog Development

The SGP4 algorithm is used to propagate ephemeris for a TLE, but does not provide covariance information. We created the covariance information by performing orbit determination on simulated measurements. Simulated ground measurements of an object (i.e., azimuth, elevation, and range) were created using the ephemeris generated by its TLE. These measurements were then processed using an extended Kalman filter. The ephemeris and covariance for each object was numerically integrated using a force model consisting of a gravity field, third-body lunar and solar perturbations, atmospheric drag (as applicable), and solar radiation pressure. The simulation was performed over a time period before 01 Oct 2011 so that the ephemeris produced over 01-03 Oct would reflect only predicted ephemeris and not any simulated measurements. This allows the covariance to grow over time.

No attempt was made to generate simulated measurements in a manner consistent with the actual collection of observations used to maintain the catalog. Every object was rich in simulated measurements, unlike the actual collection process where debris objects may have few observations. The resulting orbit determination provided excellent results with low uncertainty for every object in our simulated catalog. Three typical values are shown in Table 2. Uncertainties for actual objects can be found in practice to be up to $10\times$ larger.

Table 2. Typical initial covariance sizes in the simulated catalog.

SSC	Name	Regime	σ_{max} (m)	σ_{mid} (m)	σ_{min} (m)
24792	IRIDIUM-8	LEO	18.6	4.6	3.6
24876	NAVSTAR43	MEO	15.6	10.9	3.5
26388	TDRS-8	GEO	59.3	18.3	7.6

The resulting catalog consisted of 13,506 objects, of which 987 were GEOs. This compares well to the original set of 14,680 TLEs available for that time period. The automated orbit determination process was unable to find a satisfactory orbit for a small set of objects without more manual involvement. Our concern is conjunctions, however, and not orbit determination simulations of the entire catalog so the difference is immaterial to our needs. This simulated catalog functions as representative of the results expected when using the actual space catalog but not as actual results of the official catalog.

All-on-All Conjunction Assessment

Conjunctions were computed amongst all 13,506 objects in the catalog. The computation took 27 minutes on a 64-bit high-end engineering workstation using 24 concurrent threads. A conjunction for a pair was defined as a TCA whose range between the objects was less than 5 km. This is a typical threshold used in conjunction assessments. There were 19,541 conjunctions over the 2-day

period. We chose to model all objects as a sphere of radius 1 m rather then attempting to determine the correct size of each object[*], making $R = 2\,\text{m}$ in the probability and encounter duration computations.

A little investigation showed that 22 pairings involved slowly drifting objects which stayed within 5 km for an extended time: 21 pairings remained within 5 km for the entire 2 days while one remained close for 1.8 days. These pairings are responsible for 460 of the conjunctions. While one might expect that all the slow drifting conjunctions involve GEO objects, this is not the case: only two of the pairings involve GEO objects, with 1 pairing involving MEO objects and the remaining 19 involving LEO objects. Many of the conjunctions involved very close encounters that would be a concern for collision–see Figure 1. In each conjunction the relative speed v_0 was small, typically less than 0.1 m/s but not more than 5 m/s. The shortest encounter duration $\Delta\tau(10^{-6})$ was computed as 167 secs, while the longest was 2.3 days. Obviously, these conjunctions do not satisfy the short-term encounter assumptions–probability must be computed using a long-term encounter model.

Range Histogram

Range Bins	< 10 m	10-50 m	50-100 m	100-200 m	200-500 m	0.5-1 km	1-2 km	2-3 km	3-4 km	4-5 km
Conjunctions	23	72	33	51	155	102	2	9	6	6
Cumulative %	5%	21%	28%	39%	73%	95%	95%	97%	99%	100%
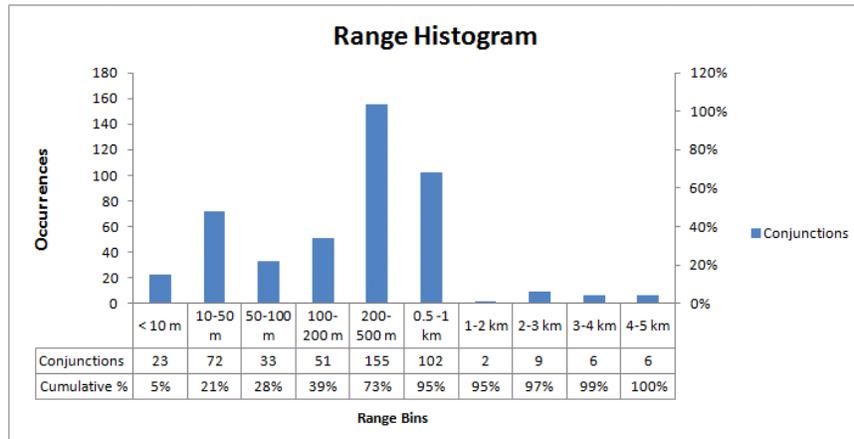
Figure 1. Range histogram for the slowly drifting objects.

Because the slowly drifting objects must be treated separately, they will be removed from further discussion. We computed the probability of collision for the remaining 19,081 conjunctions using the short-term encounter formula. A summary is provided in Table 3. Only 25 conjunctions had a probability greater than 10^{-6} and only 145 had a probability greater than 10^{-16}. The largest encounter duration of the 25 was 1.73 seconds; the largest duration of the 145 was 14.3 seconds.

More telling are the histograms of range, relative speed v_0, and the normal plane uncertainty σ_ν shown in Fig. 2, Fig. 3, and Fig. 4. Relatively few conjunctions are close: 96% have a range greater than 1 km. Over 98% of the conjunctions have a relative speed v_0 greater than 1 km/s; however, there are still 52 conjunctions with speeds less than 100 m/s. Surprisingly, 49% of the conjunctions have a normal plane uncertainty σ_ν of under 100m and 94% are under 500m.

Encounter Duration

Given the characteristics of v_0 and σ_ν, we should expect that the encounter durations will often be short. This can be seen in Fig. 5 where the duration histogram for $\gamma = 10^{-6}$ is shown. Over 95% of the conjunctions have an encounter duration of less than 0.5 seconds, and all but 33 have

---

[*]There is no known database of object sizes for the public catalog.
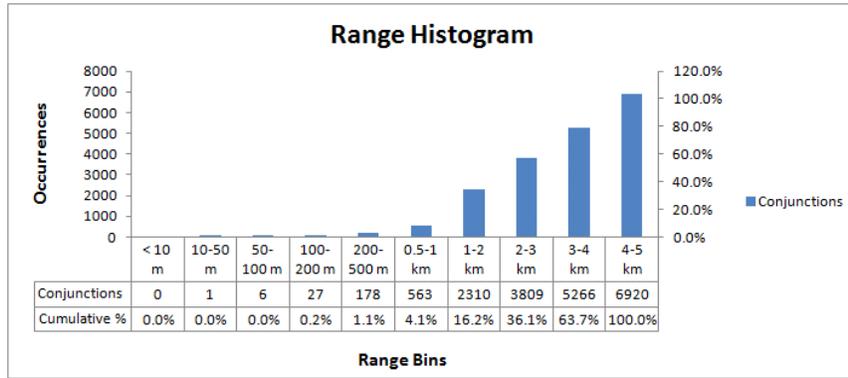
Figure 2. Range histogram.
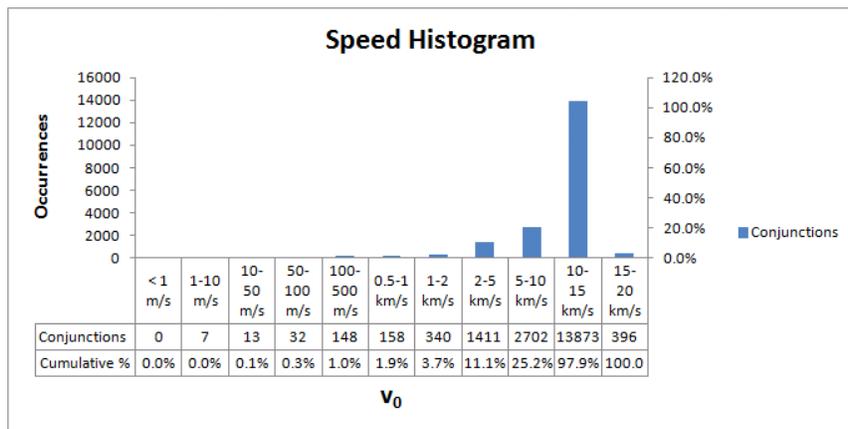
Figure 3. v_0 **histogram.**
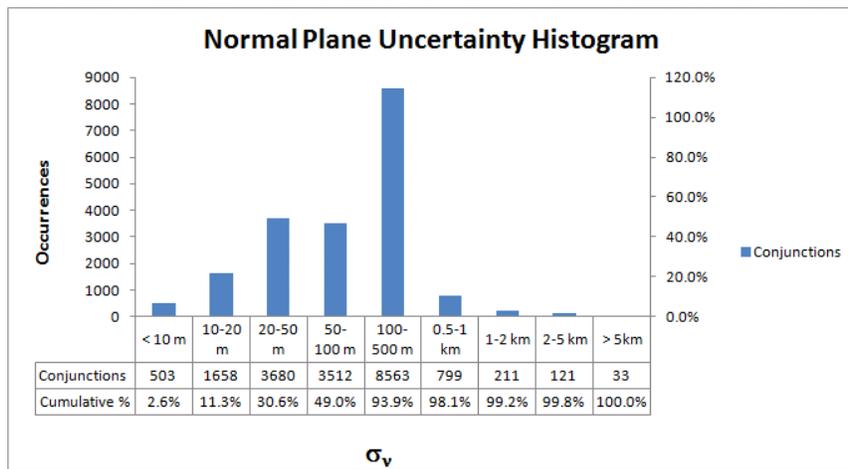
Figure 4. σ_ν **histogram.**

Table 3. Distribution of probability values.

Probability Range	Conjunctions
1.0E-04 $\leq P$	0
1.0E-05 $\leq P <$ 1.E-04	7
1.0E-06 $\leq P <$ 1.E-05	18
1.0E-08 $\leq P <$ 1.E-06	40
1.0E-10 $\leq P <$ 1.E-08	23
1.0E-12 $\leq P <$ 1.E-10	15
1.0E-14 $\leq P <$ 1.E-12	21
1.0E-16 $\leq P <$ 1.E-14	21
0.0 $\leq P <$ 1.E-16	18,935

durations less than 5 seconds. Of those 33 only 4 conjunctions involve GEO objects; 8 conjunctions involved slow encounters of LEO objects where the maximum speed was 35 m/s. The remaining 21 encounters were fast encounters (6.5 km/s $\leq v_0 \leq$ 15.5 km/s) involving LEO objects but had relatively high normal plane uncertainty (3.7 km $\leq \sigma_\nu \leq$ 39.1 km).

Even at $\gamma = 10^{-16}$, the durations do not change much. The largest duration is then 902 seconds vs. the previous maximum of 535 seconds, and 75 conjunctions have durations greater than 5 seconds. Fig. 6 shows the effect of larger initial uncertainty (i.e., $\sigma_\nu \mapsto 5\sigma_\nu$) on the encounter duration histogram. As expected, the larger the initial uncertainty the more conjunctions have durations of larger length.

Encounter Start and Stop Times

An interesting by-product of the encounter duration formula is the identification of the time interval for the encounter, i.e., $[\tau_0, \tau_1]$. Recalling that we set $t = 0$ to indicate the TCA (i.e., the reference time for evaluating v_0, $\boldsymbol{\mu}_{\zeta_0}$, and $\mathbf{A}_0$), we might expect that $t = 0$ lies on $[\tau_0, \tau_1]$. However, this only occurs for 3960 conjunctions (21%). A few conjunctions are shown in Table 4. Note that in some cases the duration $\Delta\tau$ is *smaller* than the time between the TCA at $t = 0$ and one (or both) of the encounter edges times τ_0 and τ_1.

Table 4. Some example conjunctions metrics for $\gamma = 10^{-6}$.

Regime	SSC	SSC	Range (km)	v_0 km/s	σ_ν (km)	τ_0 (s)	τ_1 (s)	$\Delta\tau$ (s)
GEO	31577	36831	2.8	0.003	0.063	-98.5	105.8	204.3
LEO	34754	34962	4.6	0.006	0.037	-147.1	-92.6	54.5
LEO	34754	34962	2.9	0.012	0.056	132.5	177.8	45.3
LEO	07363	30917	4.9	14.661	1.115	14.2	14.9	0.7
LEO	18257	35443	4.9	0.172	0.063	-9.1	-8.6	0.5
LEO	26756	35770	2.3	14.866	0.428	-0.1	0.2	0.3
LEO	34969	37438	2.5	14.791	0.167	0.3	0.5	0.2
LEO	32069	34901	3.2	14.909	0.288	-0.5	-0.4	0.1

Looking at Eq. (16a) and Eq. (16b), we see that q_0 can be of either sign whereas the the other terms in the numerators are of the same sign. Thus, q_0 is responsible for this behavior. q_0 arises from cross-correlation of the covariance matrix interacting with the relative position at TCA. It determines the time during the motion of the perturbed trajectories that the greatest contribution to $\mathcal{N}_1(\chi, 0, \sigma_\nu^2)$ is made–that time is not normally the TCA (unless, of course, the cross-correlation is zero).

Duration Histogram

	< 0.1 s	0.1-0.5 s	0.5-1 s	1-2 s	2-5 s	5-10 s	10-20 s	20-50 s	50-100 s	100-200 s	200-500 s	> 500 s
Conjunctions	9654	8574	509	225	86	16	5	6	1	1	3	1
Cumulative %	50.6%	95.5%	98.2%	99.4%	99.8%	99.9%	99.9%	100.0	100.0	100.0	100.0	100.0

Figure 5. $\Delta\tau(10^{-6})$ **histogram.**

Duration Histogram

	< 0.1 s	0.1-0.5 s	0.5-1 s	1-2 s	2-5 s	5-10 s	10-20 s	20-50 s	50-100 s	100-200 s	200-500 s	> 500 s
Conjunctions	1874	7800	5094	3100	868	225	74	28	5	4	4	4
Cumulative %	9.8%	50.7%	77.4%	93.6%	98.2%	99.4%	99.8%	99.9%	99.9%	100.0	100.0	100.0

Figure 6. $\Delta\tau(10^{-6})$ **histogram when** σ_ν **increased** $5\times$.

The formulas for τ_0 and τ_1 given by Eq. (16a) and Eq. (16b) have been derived in accordance with the short-term encounter assumption. Thus, the actual time period that the assumptions are assumed to be met is not just the encounter duration interval, but instead the larger interval Δt, the short-term encounter validity interval, defined by

$$\Delta t = \max(\Delta\tau, \|\tau_0\|, \|\tau_1\|).$$ (17)

A histogram of Δt is given in Fig. 7. There are 115 conjunctions with $\Delta t > 5$ seconds. These may merit further investigation to determine whether the short-term encounter assumptions are valid. In contrast, the encounter duration $\Delta\tau$ identified only 33 conjunctions greater than 5 seconds.

Time interval Histogram

	< 0.1 s	0.1-0.5 s	0.5-1 s	1-2 s	2-5 s	5-10 s	10-20 s	20-50 s	50-100 s	100-200 s	200-500 s	> 500 s
Conjunctions	3713	11199	2735	998	321	72	26	7	1	2	3	4
Cumulative %	19.5%	78.2%	92.5%	97.7%	99.4%	99.8%	99.9%	99.9%	100.0	100.0	100.0	100.0
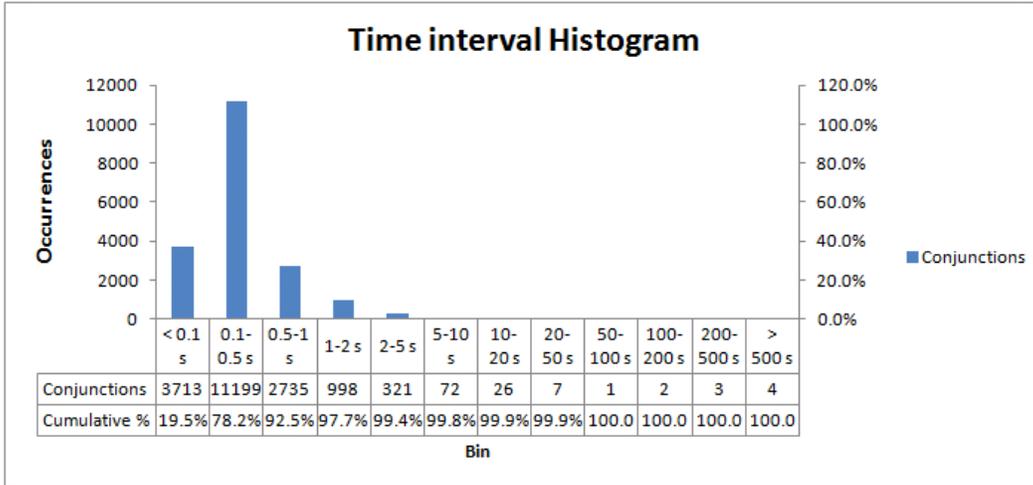
Figure 7. Δt **histogram.**

DISCUSSION

The slowly drifting objects do not satisfy the short encounter assumptions and must be assessed using other means. Many of these objects remain very close for large amounts of time. Of the remaining conjunctions, most all have a Δt value of a few seconds and (probably) satisfy the short-term encounter assumptions. The only definitive manner for determining the appropriateness of the assumption is to compare using Monte Carlo simulations but the computational effort in doing so even for one conjunctions can be daunting.[16] There are a small number of conjunctions for which Δt is more than a few seconds and it is not clear that the short term assumptions are met for these cases or not. The short-term encounter validity interval formula can be used to identify these conjunctions–they merit more investigation.

CONCLUSIONS

We have derived the formula for the encounter duration and the validity interval satisfying the short-term encounter assumptions. The encounter duration and validity interval were then computed for all conjunctions in an all-on-all conjunction assessment of a large space object catalog. While the vast majority of encounters last only a few seconds, some encounters last long enough that further investigation is warranted to determine whether the short-term assumptions are met. The the short-term encounter validity interval formula can be used to determine this small set needing investigation.

REFERENCES

[1] S. Alfano, "Determining Satellite Close Approaches," *J. Astron. Sci.*, Vol. 41, No. 2, 2005, pp. 217–225.

[2] S. Alfano, "Review of Conjunction Probability Methods for Short-term Encounters," *AAS Specialist Conference*, Sedona, AZ., Paper 07-148, Feb. 2007.

[3] S. Alfano, "A Numerical Implementation of Spherical Object Collision Probability," *J. Astron. Sci.*, Vol. 53, No. 1, 2005, pp. 103–109.

[4] K. Chan, "Collision Probability Analyses for Earth Orbiting Satellites," *Adv. Astro. Sci.*, Vol. 96, 1997, pp. 1033–1048.

[5] K. Chan, "Analytical Expressions for Computing Spacecraft Collision Probabilities," *AAS Specialist Conference*, Santa Barbara, CA., Paper 01-119, Feb. 2001.

[6] K. Chan, "Improved Analytical Expressions for Computing Spacecraft Collision Probabilities," *AAS Specialist Conference*, Ponce, Puerto Rico, Paper 03-184, Feb. 2003.

[7] K. Chan, "Short-Term vs Long-Term Spacecraft Encounters," *AIAA Conference*, Providence, RI., Paper 2004-5460, Aug. 2004.

[8] K. Chan, *Spacecraft Collision Probability*. El Segundo, CA.: The Aerospace Corporation, 2008.

[9] R. P. Patera, "General Method for Calculating Satellite Collision Probability," *AIAA J. GCD*, Vol. 24, No. 4, 2001, pp. 716–722.

[10] J. L. Foster and H. S. Estes, "A Parametric Analysis of Orbital Debris Collision Probability and Maneuver Rate for Space Vehicles," *NASA/JSC-25898*, Aug. 1992.

[11] M. R. Akella and K. T. Alfriend, "Probability of Collision Between Space Objects," *J. GCD*, Vol. 23, No. 5, 2000, pp. 769–772.

[12] V. T. Coppola, "Including Velocity Uncertainty in the Probability of Collision Between Space Objects," *AAS Specialist Conference*, Charleston, SC., Paper 12-247, Feb. 2012.

[13] S. Alfano, "Beta Conjunction Analysis Tool," *AAS/AIAA Astrodynamics Specialist Conference*, Mackinac Island, MI., Paper 07-393, Aug. 2007.

[14] R. C. Frigm and D. Rohrbaugh, "Relative Velocity as a Metric for Probability of Collision Computations," NASA GSFC IAC-08-A6.2.5, 2008.

[15] Z. N. Khutorovsky, V. F. Boikov, and S. Y. Kamensky, "Direct Method for the Analysis of Collision Probability of Artificial Space Objects in LEO: Techniques, Results, and Applications," *Proc. First European Conf. on Space Debris*, Apr. 1993, pp. 491–508.

[16] S. Alfano, "Satellite Conjunction Monte Carlo Analysis," *AAS Spaceflight Mechanics Mtg*, Pittsburgh, PA., Paper 09-233, Feb. 2009.